PAPER • OPEN ACCESS

Uncertainty Quantification of Turbulence Model Applied to a Cavitating Hydrofoil

To cite this article: Simone Romani *et al* 2023 *IOP Conf. Ser.: Mater. Sci. Eng.* **1288** 012037

View the article online for updates and enhancements.

Uncertainty Quantification of Turbulence Model Applied to a Cavitating Hydrofoil

Simone Romani, Mitja Morgut, Lucia Parussini

Department of Engineering and Architecture, University of Trieste, 34127 Tieste, Italy

E-mail: `simone.romani@phd.units.it, mmorgut@units.it, lparussini@units.it`

Abstract. This paper presents the Global Sensitivity Analysis of the coefficients of the standard k-ε turbulence model used in RANS (Reynolds Averaged Navier-Stokes) simulations aimed to predict the flow around a bi-dimensional hydrofoil operating at non-cavitating and cavitating flow regimes. The sensitivity analysis is treated by the Sobol Decomposition, where the Sobol Indices are computed through the Polynomial Chaos Expansion of the 2-nd order with a Point-Collocation Non-Intrusive approach. From the current results, it seems that the considered cavitating flow regime is less sensitive to the variability of the input parameters, at least for the prediction of lift and drag.

1. Introduction
Owing to the continuous improvements of the CFD (Computational Fluid Dynamics) technologies and continuous increase of the computer performances, numerical simulations are today extensively used for design purposes, allowing the experimental test to be performed only at the final stages of the project. But, despite the progress of the computational technologies, the uncertainties related to the operative conditions, the geometry (due to manufacture tolerances) as well as the physical model can still affect the reliability of a CFD-based design procedure.

In this work, we focus on the uncertainties related to a physical model. In particular, we investigate, using a stochastic approach, based on the Polynomial Chaos Expansion, the possible influence of the propagation of the uncertainties imposed on the coefficients of the standard k-ε turbulence model on the prediction of the lift and drag forces of a NACA66(MOD) hydrofoil operating at a given angle of attack [1].

The study is carried out for a selected cavitating flow regime as well as for the fully-wetted flow condition. The flow is treated as a homogeneous mixture of water and vapour, and the mass transfer rate is modelled using the Zwart et al. model [2].

At this stage, it is important to point out that uncertainties can be classified into two families: *aleatory uncertainties*, which describe the natural/intrinsic variability of a certain quantity; *epistemic uncertainties*, which depend closely on the set of knowledge available [3].

Moreover, the Sensitivity Analysis which allows to quantify the contribution of the uncertainties related to given model inputs (as turbulence model coefficients considered in this study, for instance) to the uncertainty of the model output (as lift and drag evaluated in this study, for instance) can be preformed using two different approaches: *Local Sensitivity Analysis*, which analyses the effects of local changes of a parameter in a system; *Global Sensitivity Analysis*, which evaluates the entire parameter space and the contribution of input variables to the outputs.

Here, a Global Sensitivity Analysis has been carried out, relying on the Variance Based Method and Sobol Decomposition.

Using such an approach, the importance of a given input parameter x_i to the uncertainty of the specific response y is measured using *variance* as a yardstick. Then, Sobol indices are used to rank the influence of input parameters, as well as its combination, on the predictions of selected output parameters. [3, 4, 5, 6]

In this study, as previously mentioned, the uncertainty propagation and the Sobol Indices for the sensitivity analysis have been determined exploiting a method based on response surfaces. Specifically, the Polynomial Chaos Expansion based on a Point-Collocation Non-Intrusive Approach [7, 8].

The selected approach has been practically implemented using *Dakota*, an optimization and uncertainty quantification framework [9], in combination with *Ansys-CFX*, a general purpose CFD (Computational Fluid Dynamics) solver [10]. In particular, Dakota has been used to evaluate the random values of the input coefficients as well as the values of the Sobol Indices, while Ansys-CFX has performed the required simulations.

From the overall results, it seems that the uncertainty propagates differently for the two selected flow regimes. As a matter of fact, the variance of the global values (lift and drag) observed in the cavitating flow regime is less than that obtained for the fully-wetted flow conditions. Moreover, from the comparison of the Sobol indices it seems that the ranking of the contributions of the single input parameters to the uncertainty is also different, as well as the ranking of the contributions of mutual parameter interactions.

In the following, the approach for the uncertainty quantification and sensitivity analysis is described. Then, for the sake of clarity the standard $k - \varepsilon$ turbulence model is presented along with the mathematical model for the cavitating flow. Next, the computational strategy is presented. Finally the results are discussed and concluding remarks are provided.

2. Uncertainty Quantification and Sensitivity Analysis
As introduced in the above section, the importance of the turbulence model coefficients has been quantified by Sobol Indices. Thus, for the sake of completeness, a brief description in accordance with [6, 11] is given in the following.

Since the Sobol Indices are composed by total and partial variances, we start by defining the total variance, D, named also Global Sensitivity as:

$$D = \text{Var}\left\{f\left(\underline{x}\right)\right\} = \int_{K^n} f^2\left(\underline{x}\right) d\underline{x} - f_0^2, \tag{1}$$

where:

$$K^n = \left\{\underline{x} : 0 \le x_i \le 1 \, , \, i = 1, \dots, n\right\} : n - \text{dimensional unit cube} \tag{2}$$

and generalized response:

$$f\left(\underline{x}\right) = f\left(x_1, \dots, x_n\right) = f_0 + \sum_{i=1}^{n} f_i\left(x_i\right) + \sum_{1 \le i < j \le n}^{n-1} \left[f_{ij}\left(x_i, x_j\right) + \dots + f_{1, \dots, n}\left(x_1, \dots, x_n\right)\right]. \tag{3}$$

Now, the total variance can be decomposed as:

$$D = \sum_{i=1}^{n} D_i + \sum_{1 \le i < j \le n}^{n-1} \left[D_{ij} + \dots + D_{1, \dots, n}\right], \tag{4}$$

where, the partial variances in (4) are specified in the below equation:

$$D_{i_1, \ldots, i_s} = \int_{K^s} f^2_{i_1, \ldots, i_s} (x_{i_1}, \ldots, x_{i_s}) \, dx_{i_1}, \ldots, dx_{i_s} \quad \text{for } 1 \le i_1 < \ldots < i_s \le n \text{ and } s = 1, \ldots, n. \quad (5)$$

Sobol's Indices are defined as follows:

$$S_{i_1, \ldots, i_s} = \frac{D_{i_1, \ldots, i_s}}{D} \quad (6)$$

and by the total variance decomposition, the indices satisfy the property:

$$\sum_{i=1}^{n} S_i + \sum_{1 \le i < j \le n}^{n-1} [S_{ij}, \ldots, S_{1, \ldots, n}] = 1. \quad (7)$$

At this stage, it is important to point that, $S_{i_1}, \ldots, S_{i_s}$ are useful for studying uncertainty because they classify which amount of the total variance is influenced by the uncertainties in the set of input parameters $\{i_1, \ldots, i_s\}$.

Instead, $\sum_{i=1}^{n} S_i$ are first order terms which measure the influence of each parameter taken alone without taking into account mutual interactions.

On the other hand higher order indices evaluate the possible mixed influence of various parameters.

2.1. Polynomial Chaos Expansion

The Polynomial Chaos Expansion is a non-sampling-method capable of determining the evolution of uncertainty in a dynamic system, where random functions or random variables are expressed in deterministic and aleatory components. It is based on the spectral representation of uncertainties.

In practice an output response of a model can be approximated/expressed in truncated polynomial form [8]. The goal is to evaluate the polynomial coefficients because they give a measure of the uncertainties and allow us to perceive which input variables weight more on the response function [12]. The coefficients can be determined by an intrusive or non-intrusive approach on the original equations .

This work is based on the Point-Collocation Non-Intrusive Polynomial Chaos approach [7]. In the case of the PCE the Sobol indices can be evalutated as:

$$D = \sigma^2 \left[Y \left(t, \underline{\xi} \right) \right] = \sum_{i=1}^{M} \alpha_i^2 (t) = \sum_{i=1}^{M} \sum_{k=1}^{K} Y^2 (t, \xi_k) \, \varphi_i^2 (\xi_k) \, w_k^2, \quad (8)$$

where:

- $\underline{\xi} = (\xi_1, \ldots, \xi_K)$: set of K random variables
- $\varphi_i(\xi_k)$: i-th basis function with respect to the k-th random variable
- $Y(t, \xi_k)$: stochastic process associated with the k-th random variable
- $\alpha_i(t)$: i-th Polynomial Chaos coefficient
- w_k: k-th weight.

In this work, we have considered a continuous uniform distribution function so that basis functions are Legendre polynomials [13] and all weights, w_k, are equal to 1. Then, Polynomial Chaos coefficients are directly evaluated solving the system:

$$\begin{Bmatrix} Y(t,\xi_1) \\ \vdots \\ Y(t,\xi_K) \end{Bmatrix} = \begin{bmatrix} \varphi_0(\xi_1) & \cdots & \varphi_M(\xi_1) \\ \vdots & \ddots & \vdots \\ \varphi_0(\xi_K) & \cdots & \varphi_M(\xi_K) \end{bmatrix} \begin{Bmatrix} \alpha_0(t) \\ \vdots \\ \alpha_M(t) \end{Bmatrix}. \tag{9}$$

3. Mathematical model for cavitating flow

The cavitating flow has been modelled as a homogeneous mixture flow (liquid-vapour mixture) governed by the following continuity, momentum and volume fraction transport equations:

$$\nabla \cdot \underline{v} = \dot{m} \left(\frac{1}{\rho_l} - \frac{1}{\rho_v} \right) \tag{10}$$

$$\frac{\partial}{\partial t} (\rho \underline{v}) + \nabla \cdot (\rho \underline{v}\underline{v}) = -\nabla p + \nabla \cdot \left\{ (\mu + \mu_t) \left[\nabla \underline{v} + (\nabla \underline{v})^T \right] \right\} \tag{11}$$

$$\frac{\partial \gamma}{\partial t} + \nabla \cdot (\gamma v) = \frac{\dot{m}}{\rho_l} \tag{12}$$

with: $\underline{v}$, time averaged mixture velocity, p time averaged pressure, $\dot{m}$ interphase mass transfer rate due to cavitation, ρ_v vapour density, ρ_l liquid density, μ_t turbulent viscosity. The vapour α and water volume fractions are defined as:

$$\gamma = \frac{V_{liquid}}{V_{total}} \qquad \alpha = \frac{V_{vapour}}{V_{total}}$$

which relates as:

$$\gamma + \alpha = 1. \tag{13}$$

and the mixture density, ρ, and mixture viscosity, ν are defined as:

$$\rho = \gamma \rho_l + (1 - \gamma) \rho_v \tag{14}$$

$$\mu = \gamma \mu_l + (1 - \gamma) \mu_v. \tag{15}$$

Furthermore, in order to close the system of the governing equation, the standard k-ε turbulence model and the native CFX mass transfer model, i.e. the Zwart et all model, are employed to evaluate the turbulent viscosity, μ_τ, and the mass transfer rate, $\dot{m}$, respectivelly.

3.1. Zwart et al. model
The Zwart model is based on the simplified Rayleigh-Plesset equation for bubble dynamics:

$$\dot{m} = \begin{cases} -F_e \dfrac{3 r_{nuc}(1-\alpha)\rho_v}{R_B} \sqrt{\dfrac{2}{3}\left(\dfrac{p_v - p}{\rho_l}\right)}, & \text{if } p < p_v \\[4mm] F_c \dfrac{3\alpha \rho_v}{R_B} \sqrt{\dfrac{2}{3}\left(\dfrac{p - p_v}{\rho_l}\right)} & \text{if } p > p_v, \end{cases} \tag{16}$$

where p_v is vapour pressure, $r_{nuc} = 5.0 * 10^{-4}$ nucleation site volume fraction, $R_B = 1.0 * 10^{-6}$ radius of a nucleation site. $F_e = 300$ and $F_c = 0.03$ empirical calibration coefficient set according to [2].

3.2. Standard k-ε turbulence model

As pointed out previously, in order to evaluate the turbulent viscosity:

$$\mu_t = \rho C_\mu \frac{k^2}{\varepsilon}$$

(17)

the standard k-ε model has been employed [14].

In the following the governing equations of the turbulence model along with the standard model constants, subsequently modified by the sensitivity analysis, are presented.

$$\frac{\partial}{\partial t} (\rho k) + \nabla \cdot (\rho \underline{v} k) = \nabla \cdot (\mu_{eff,k} \nabla k) + P_k - \rho \varepsilon = \nabla \cdot (\mu_{eff,k} \nabla k) + S^k$$

(18)

$$\frac{\partial}{\partial t} (\rho \varepsilon) + \nabla \cdot (\rho \underline{v} \varepsilon) = \nabla \cdot (\mu_{eff,\varepsilon} \nabla \varepsilon) + C_{\varepsilon 1} \frac{\varepsilon}{k} P_k - C_{\varepsilon 2} \frac{\varepsilon^2}{k} \rho = \nabla \cdot (\mu_{eff,\varepsilon} \nabla \varepsilon) + S^\varepsilon,$$

(19)

The above equations are the turbulent kinetic energy and turbulent energy dissipation rate transport equations, and where

$$\mu_{eff,k} = \mu + \frac{\mu_t}{\sigma_k} \quad , \quad \mu_{eff,\varepsilon} = \mu + \frac{\mu}{\sigma_\varepsilon}$$

.

P_K is the production of turbulent energy term. In Table 1 the native values of the model coefficients are provided.

Table 1. Calibration constants of the Standard k-ε Model

Constant	Native value
$C_{\varepsilon 1}$	1.440
$C_{\varepsilon 2}$	1.920
C_μ	0.090
σ_k	1.000
σ_ε	1.300

4. Computational strategy

In this section the logic employed to perform the uncertainty quantification and sensistivity analysis is first described. Then, the numerical setup used to performed the numerical simulations, required by the PCE method, is presented.

4.1. Logic

The PCE method has been applied taking advantage of Dakota. In this case, the study has been practically performed in three separate stages.

Stage 1: Using Dakota, the collocation points (samplings) for the deterministic CFD simulations were generated using Latin Hypercube Sampling (LHS). In this study, the number of the collocation points, N_s, was set following [9] and for the second order of the polynomial chaos expansion.

$$N_s = n_p \left[\frac{(n+p)!}{n!p!} \right]$$

(20)

In the above equation p is the order of the polynomial expansion, n_p is the oversampling ratio, n is the number of the uncertain variables. Here: $p = 2$, $n_p = 2$, $n = 5$, thus $N_s = 42$.

The 12th International Workshop on Ship and Marine Hydrodynamics

IOP Conf. Series: Materials Science and Engineering   1288 (2023) 012037

IOP Publishing

doi:10.1088/1757-899X/1288/1/012037

Stage 2: The overall CFD simulations were carried out for the given set of collocation points. The related results were saved in proper text files.

Stage 3: Using again Dakota, in combination with a proper and ad-hoc implemented interface, the polynomial chaos coefficients were determined based on the results obtained at stage 2. The related probabilistic values as well as sensitivity indices were calculated.

Fo the sake of clarity, it is important to point out that the overall computational strategy was subdivided in three separate stages in order to perform the CFD simulation independently from Dakota which was conveniently used at the first and third stages.

4.2. CFD setup
As pointed out previously, the current study has been performed considering the NACA66MOD hydrofoil at angle of attack of 4 degrees. The hydrofoil had camber ratio $f/c = 0.020$, mean line $a = 0.8$, thickness ratio t/c=0.9, and chord c=0.150. In the above fractions f is the maximum thickness, t maximum camber.

In order to simulate the turbulent bi-dimensional flow the computational domain depicted in Figure 1 has been used.

Figure 1. Geometry of the domain and boundary conditions
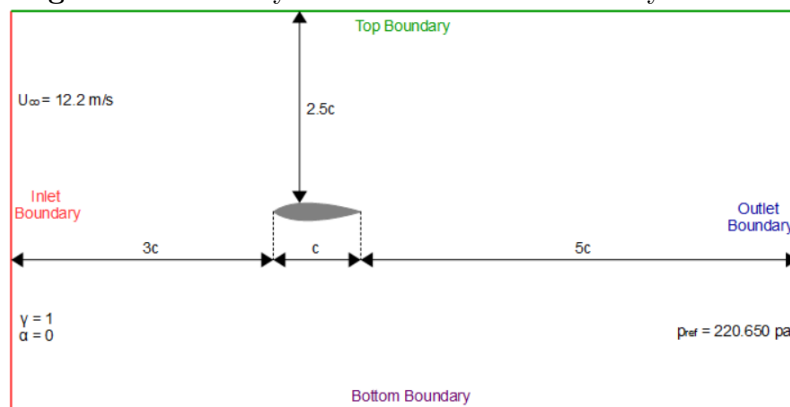
For all the simulations the free-stream velocity imposed at inlet boundary has been kept equal to U=12.2 m/s, as well as the values of the turbulent kinetic energy $k = 0.0223$ m^2/s^2 and turbulent dissipation rate $\varepsilon = 0.1837$ m^2/s^3. The pressure on outlet boundary, P_{out} has also been kept constant, in this case equal to 202650 Pa. For this reason in order to simulate, respectively, the fully wetted-flow and and the selected cavitating flow regime - in this case $\sigma = (P_{out} - P_v)/(0.5\rho_L U^2) = 0.91$ - the value of the vapour pressure, P_v, has been properly modified. The water density has been set equal to $\rho_L = 998$ kg/m^3 and maximum water-vapour density ratio has been limited to $\rho_L/\rho_V = 1000$ in order to ensure solver stability.

The simulations have been carried out using a steady state approach, on a hexa-structured mesh with about 58.7k nodes which proved to ensure mesh independent results [2]. The average value of y^+ on hydrofoil surface, evaluated considering the fully wetted flow regime, was equal to 28.

5. Results
The computational strategy, described in the former section, has been practically used considering the variability of the model coefficients within own sensitivity intervals. As first point of reference, the ranges described in [15] and the Pope equation for σ_ε have been taken into account (see Table 2 and eq. (21))

$$\sigma_\varepsilon = \frac{k^2}{C_\mu^{\frac{1}{2}} \left(C_{\varepsilon_2} - C_{\varepsilon_1}\right)} \tag{21}$$

Table 2. First Intervals of k-ε coefficients

Coefficient	L. Bound	U. Bound	Interval
C_μ	0.0500	0.150	0.100
σ_k	0.800	1.400	0.600
C_{ε_1}	1.000	1.500	0.500
C_{ε_2}	1.500	3.000	1.500
σ_ε	0.290	1.500	1.210

It is important to point out that in the preliminary study, carried out considering the intervals reported in Table 2, several simulations run to overflow. For this reason, the sensitivity intervals have been properly reduced as shown in Table 3.

Table 3. Final Intervals of k-ε coefficients

Coefficient	L. Bound	U. Bound	Interval
C_μ	0.0634	0.146	0.0826
σ_k	0.840	1.365	0.525
C_{ε_1}	1.064	1.464	0.400
C_{ε_2}	1.561	3.000	1.439
σ_ε	1.300	1.300	0.000

5.1. Hydrodynamics Characteristics

As for hydrodynamic coefficients, from Table 4 it is possible to note that the standard deviation, σ_{std}, is very low regardless of the flow regime. The predicted mean values, m, of lift and drag are, in this case, in line with the results obtained with the native values of the turbulence model coefficients [2]. However, the predictions of lift and drag for the cavitating flow regime seems to be less influenced by the variability (uncertainty) of the input parameters.

Table 4. Mean value and standard deviation of C_D and C_L

H. coefficient	Condition	m	σ_{std}
C_D	no cavitation	$2.266 \cdot 10^{-2}$	$5.781 \cdot 10^{-3}$
C_D	cavitation	$1.764 \cdot 10^{-2}$	$1.804 \cdot 10^{-6}$
C_L	no cavitation	$6.499 \cdot 10^{-1}$	$1.137 \cdot 10^{-2}$
C_L	cavitation	$6.533 \cdot 10^{-1}$	$3.512 \cdot 10^{-5}$

5.2. Sobol indices

Here, the Sobol indices are first presented separately for the two different flow regimes and next, some consideration regarding the comparison between the obtained results is given.
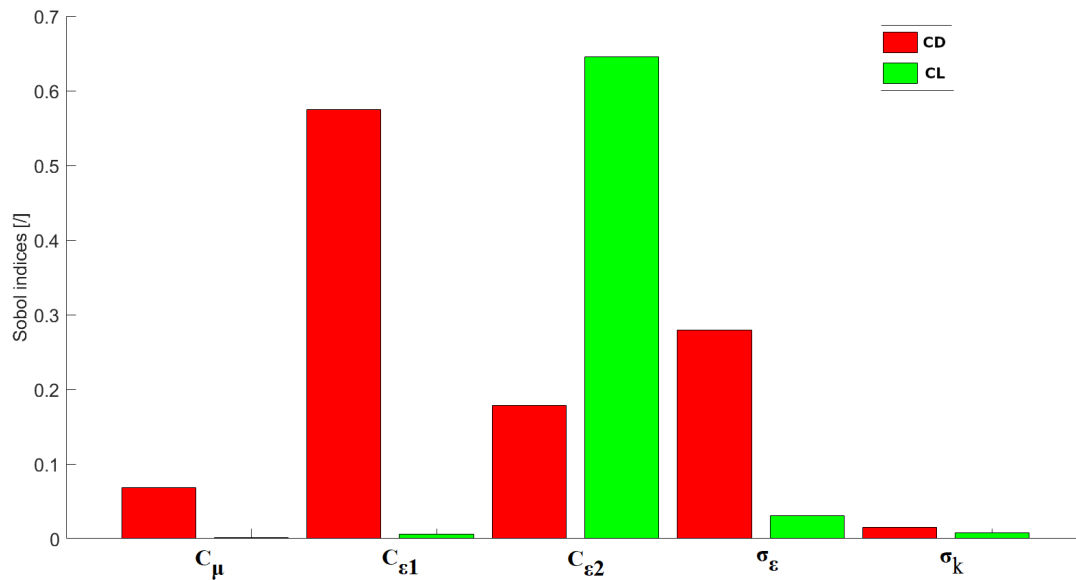
Non cavitating flow

Figure 2. Comparison between the mean values of Sobol indices for C_D and C_L in non cavitating case, for a Polynomial Chaos of the second order
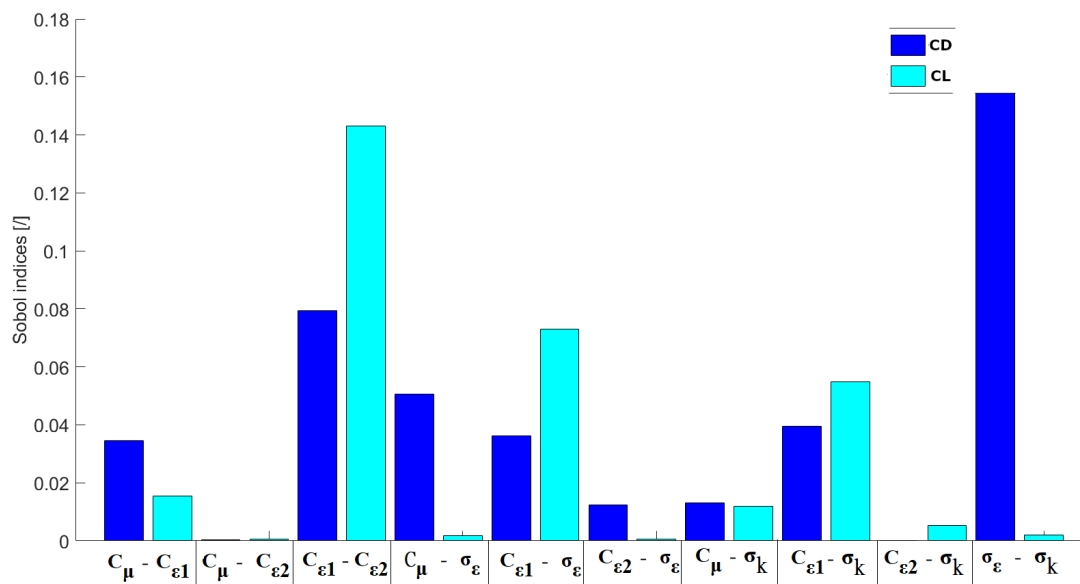

Figure 3. Comparison between interactions (pairs) of Sobol indices for C_D and C_L in non cavitating case, for a Polynomial Chaos of the second order

From Figure 2 it is possible to note that drag is most influenced by C_{ε_1}, while lift is most influenced by C_{ε_2}. Figure 3 shows that $\sigma_\varepsilon - \sigma_k$ is the pair that most influences the prediction of drag and $C_{\varepsilon_1} - C_{\varepsilon_2}$ is the pair that most influences the lift.
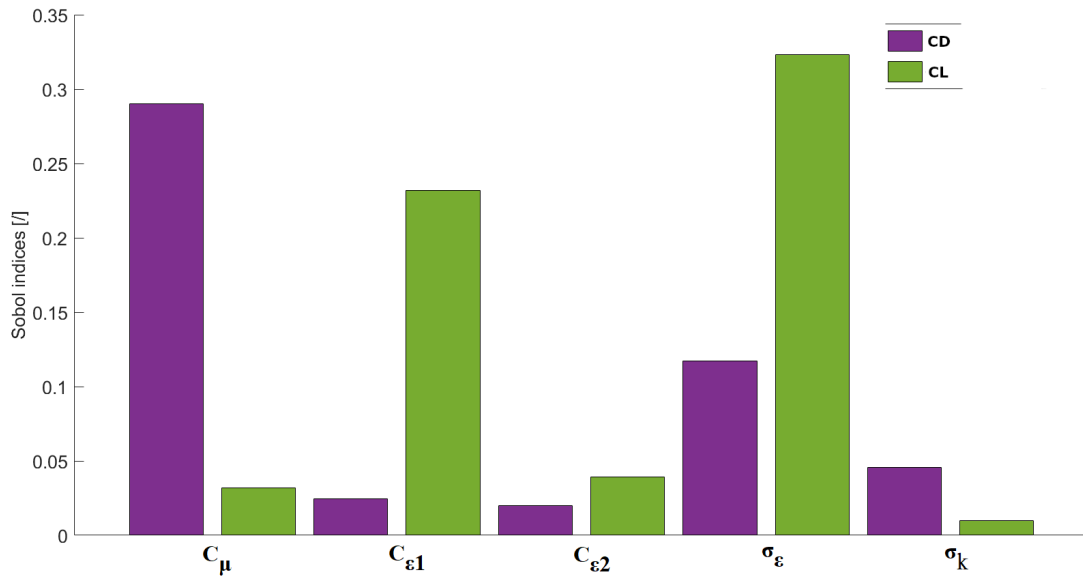
Cavitating flow

Figure 4. Comparison between the mean values of Sobol indices for C_D and C_L in cavitating case, for a Polynomial Chaos of the second order
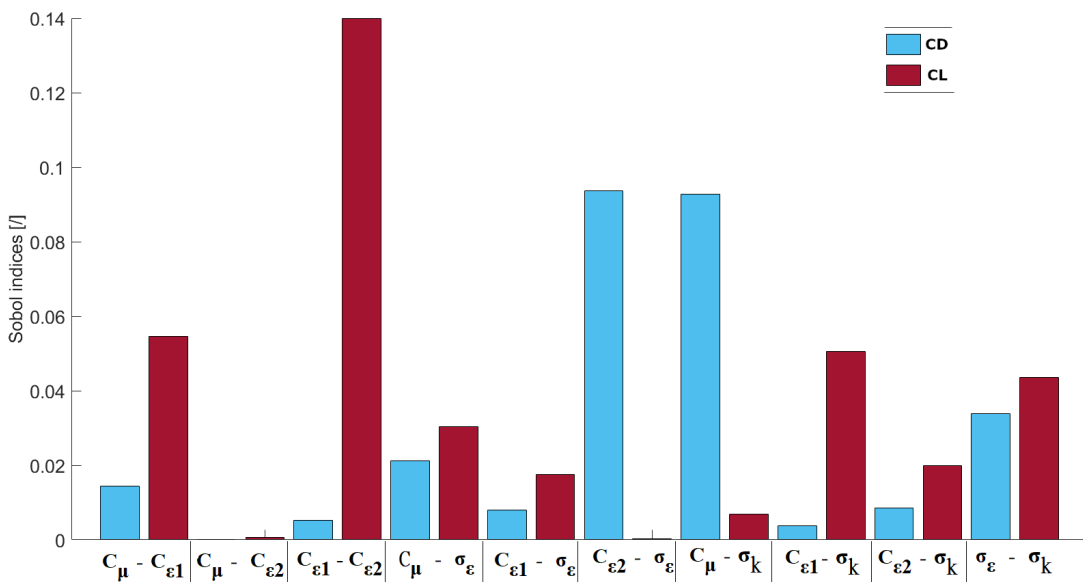

Figure 5. Comparison between interactions (pairs) of Sobol indices for C_D and C_L in cavitating case, for a Polynomial Chaos of the second order

From Figure 4 it is possible to note that drag is most influenced by C_μ, while lift is most influenced by C_{ε_1} and σ_ε. Figure 5 shows that $c_{\varepsilon_2} - \sigma_\varepsilon$ and $C_\mu - \sigma_k$ are the pair that most influence the prediction of drag and $C_{\varepsilon_1} - C_{\varepsilon_2}$ is the pair that most influences the lift.

Moreover considering Figures 2 - 4 it is possible to observe that for lift as well as drag the most important coefficients are different for the two different flow regimes. Eventually comparing Figures 3 and 5 the same behaviour can be observed for mutual interactions.

6. Conclusions

In this study, the Global Sensitivity Analysis has been applied to the case of the RANS simulations of the flow around the NACA66(MOD) hydrofoil operating at a given angle of attack. In particular, for non cavitating and cavitating flow regimes the possible effect of the uncertainties of the coefficient of the standard $k - \varepsilon$ turbulence model on the predicted lift and drag coefficients has been evaluated.

The uncertainty propagation and the Sobol Indices for the sensitivity analysis have been determined using the Polynomial Chaos Expansion, of the second order, based on a Point-Collocation Non-Intrusive Approach.

The solution strategy has been based on Dakota, which has been employed to evaluate the random values of the input coefficients as well as the values of the Sobol Indices, while Ansys-CFX has been used to perform the required simulations.

From the obtained results it seems that, for the considered flow conditions and with the considered ranges for uncertainties, the hydrodynamic characteristics are less sensitive to the variability of the turbulence model coefficients for the cavitating flow condition than for the non-cavitating flow regime. Moreover, considering the ranking based on Sobol indices, it seems that the most important input parameters are related to the given output (lift or drag) as well as to the considered flow regime. The same trend has been observed for parameter interactions.

7. References

[1] Shen Y T and Dimotakis P E 1989 The influence of surface cavitation on hydrodynamic forces *Proc. 22nd ATTC, St. Johns, Canada* pp 44–53
[2] Morgut M, Nobile E and Biluš I 2011 *International Journal of Multiphase Flow* **37** 620–626
[3] Zhang J, Yin J and Wang R 2020 *Mathematical Problems in Engineering* **2020**
[4] Eck V G, Donders W P, Sturdy J, Feinberg J, Delhaas T, Hellevik L and Hunberts W 2015 *International Journal for Numerical Methods in Biomedical Engineering* **32** 1–32
[5] Pathmanathan P, Cordeiro J and Gray R 2019 *Frontiers in Physiology* **10**
[6] Sudret B 2008 *Reliability Engineering and System Safety* **93** 964 – 979
[7] Hosder S and Walters R *Computattional Uncertainty in Military Vehicle Design*
[8] Kaintura A, Dhaene T and Spina D 2018 *Electronics* **7**
[9] Adams B M, Bohnhoff W J, Dalbey K R, Ebeida M S, Eddy J P, Eldred M S, Hooper R W, Hough P D, Hu K T, Jakeman J D, Khalil M, Maupin K A, Monschke J A, Ridgway E M, Rushdi A A, Seidl D T, Stephens J A, Swiler L P and Winokur J G 2020 *Dakota, A Multilevel Parallel Object-Oriented Framework for Design Optimization, Parameter Estimation, Uncertainty Quantification, and Sensitivity Analysis: Version 6.13 User's manual* Sandia National Laboratories
[10] URL www.ansys.com
[11] Katsuno E, Lidtke A, Düz B, Rijpkema D, Dantas J and Vaz G *Computers and Fluids* **230** 16
[12] Mourousias N, García-Gutiérrez A, Malim A, Fernández D, Marinus B and Runacres M 2022 *Aerospace Science and Technology* **133** 16
[13] Doma B 2015 *The classical Orthogonal Polynomial* (Singapore)
[14] Moukalled F, Mangani L and Darwish M 2015 *The Finite Volume Method in Computational Fluid Dynamics* vol 113
[15] Shirzadi M, Mirzaei P and Naghashzadegan M 2017 *Journal of Wind Engineering and Industrial Aerodynamics* **171** 366 – 379